

# Anharmonic effect on the equation of state (EoS) for NaCl

Tatsuya Sumita · Akira Yoneda

Received: 11 April 2013 / Accepted: 16 September 2013 / Published online: 16 October 2013  
© The Author(s) 2013. This article is published with open access at Springerlink.com

**Abstract** We find clear intrinsic anharmonicity in the NaCl-B1 phase by examining the equation of state (EoS) based on previous ultrasonic velocity data for pressures up to 0.8 GPa and temperatures up to 800 K. The experimental EoS for this phase shows that its specific heat at constant volume ( $C_V$ ) is significantly smaller than that based on a harmonic model. Also, the sign of  $(\partial C_V / \partial P)_T$ , which is normally negative in the quasi-harmonic approximation, is unexpectedly positive. The thermodynamic Grüneisen parameter ( $\gamma$ ), which has frequently been assumed to be a single-variable function of molar volume, shows not only volume dependence but also negative temperature dependence. To understand these features of  $C_V$  and  $\gamma$ , we introduce a thermodynamic model including positive quartic anharmonicity. To make an anharmonic model advancing the ordinarily quasi-harmonic approximation model, we introduce two parameters: anharmonic characteristic temperature ( $\theta_a$ ) and its volume derivative. In the anharmonic model, the value of  $C_V$  is calculated along an isochore using classical statistical mechanics and a harmonic quantum correction. At high temperatures, the decrease in  $C_V$  from the Dulong-Petit limit is related to the value of  $T/\theta_a$ . For infinitely large  $\theta_a$ , the system is

approximately quasi-harmonic. The temperature dependence of  $\gamma$  is related to  $C_V$  by the thermodynamic identity  $(\partial C_V / \partial \ln V)_T = C_V (\partial \gamma / \partial \ln T)_V + \gamma (\partial C_V / \partial \ln T)_V$ . Even though our modification of the quasi-harmonic approximation is simple, our anharmonic model succeeds in reproducing the experimental  $\gamma$  and  $C_V$  simultaneously for the NaCl-B1 phase.

**Keywords** Complete travel-time equation of state (CT-EoS) · Intrinsic anharmonicity · Thermodynamic model · Statistical mechanics · NaCl-B1 phase · Grüneisen parameter

## Introduction

The equation of state (EoS) for the NaCl-B1 phase is representative of pressure scales up to approximately 25 GPa. In particular, Decker's (1971) EoS is based on both lattice dynamics and the quasi-harmonic Debye model and has frequently been used for more than 30 years in high-pressure experiments in solid-state physics, geophysics, and material sciences. However, Decker's (1971) EoS cannot reproduce the corresponding zero-pressure thermodynamic properties (e.g., thermal expansion coefficient  $\alpha(0, T)$  and isobaric specific heat  $C_p(0, T)$ ; compare the thin solid line with the connected circles in Fig. 1). Later, Brown (1999) reported an EoS that was consistent with experimental  $\alpha(0, T)$  data. However, the  $C_p(0, T)$  values are still significantly inconsistent with experiment (see dashed line in Fig. 1). These two EoSs commonly assume both the quasi-harmonic Debye model and a  $\gamma$  value that is dependent solely on molar volume, i.e.,  $\gamma = \gamma(V)$ .

Spetzler et al. (1972) found experimental support for the  $\gamma = \gamma(V)$  hypothesis. They measured the ultrasonic velocity

**Electronic supplementary material** The online version of this article (doi:10.1007/s00269-013-0627-z) contains supplementary material, which is available to authorized users.

T. Sumita (✉)  
Geological Survey of Japan, National Institute of Advanced  
Industrial Science and Technology (AIST), Tsukuba,  
Ibaraki 305-8567, Japan  
e-mail: t.sumita@aist.go.jp

A. Yoneda  
Institute for Study of the Earth's Interior, Okayama University,  
Misasa, Tottori 682-0193, Japan

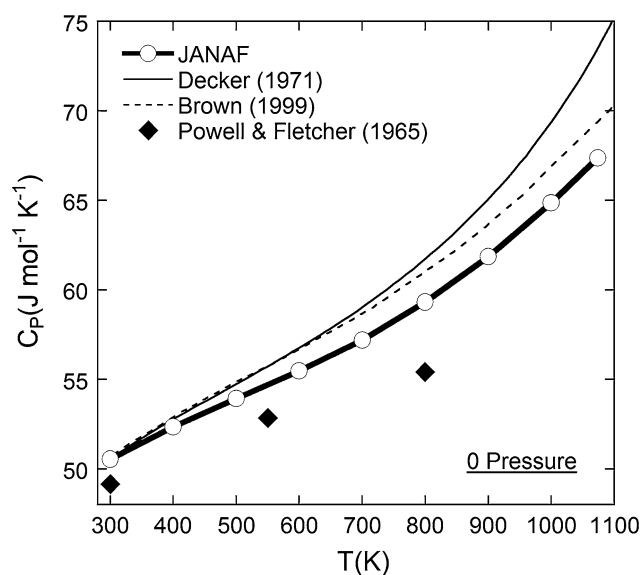


**Fig. 1** Comparison of the isobaric specific heat at zero pressure. **Bold line with circles** experimental values compiled by Chase (1998); **thin solid line** Decker (1971) EoS; **dashed line** Brown (1999) EoS; **diamonds** theoretical values of Powell and Fletcher (1965) as used in Spetzler et al. (1972)

at zero pressure and 300 K,  $v_i(0, 300\text{K})$ , and the frequency (normalized inverse travel time) up to 0.8 GPa and 800 K,  $F_i(P, T)$ , and then calculated major thermodynamic quantities including  $\gamma$  from the ultrasonic data combined with  $\alpha(0, T)$  and  $C_p(0, T)$ . Spetzler and Yoneda (1993) refer to this calculated result as the complete travel-time equation of state, or CT-EoS. However, we have ascertained that Spetzler et al. (1972) calculated the CT-EoS using  $C_p(0, T)$  values based on a theoretical model (Powell and Fletcher 1965) that yields values 7 % smaller than the experimental (Chase 1998) at 800 K (see Fig. 1). These unsatisfactory  $C_p$  values cause significant uncertainty in  $\gamma$ , because  $\gamma = \alpha V K_S / C_p$  (where  $K_S$  is the adiabatic bulk modulus).

Therefore, first of all, we recalculate the CT-EoS with experimental  $C_p(0, T)$  data instead of the theoretical values of Powell and Fletcher (1965). The result gives a  $\gamma$  value that shows not only volume but also temperature dependence, in contrast to the original result of Spetzler et al. (1972). At high temperatures, the specific heat at constant volume ( $C_V$ ) in the CT-EoS is smaller than that obtained using a harmonic approximation where the difference exceeds the expected tolerance. These inconsistencies clearly suggest the limitation of harmonic or quasi-harmonic approximation. Thus, we consider introducing intrinsic anharmonicity.

The importance of intrinsic anharmonicity to thermodynamic properties of NaCl or similar materials such as MgO is already recognized (e.g., Leadbetter et al. 1969; Cowley 1971; Stacey and Isaak 2003; Oganov and Dorogokupets

2003, 2004). Others have recently proposed NaCl EoSs including intrinsic anharmonicity (e.g., Dorogokupets 2002; Dorogokupets and Dewaele 2007). These papers treat the intrinsic anharmonic effect on  $C_V$  as a linear function of temperature, which is the simplest approximation neglecting higher orders in series expansion of the anharmonic Helmholtz free energy. However, these EoSs commonly fail to reproduce  $\gamma$  in spite of fair reproduction of  $C_V$  or  $C_p$ .

Nextly, we present a new thermodynamic model for  $C_V$  and  $\gamma$  that takes account of the intrinsic anharmonic effect. First, we consider positive quartic anharmonicity under an isochoric condition. Classical statistical mechanics is directly used instead of the series approximation (Leadbetter et al. 1969; Oganov and Dorogokupets 2003, 2004; Dorogokupets 2002; Dorogokupets and Dewaele 2007), which inevitably causes uncertainty by neglecting higher-order terms. We express the temperature dependence of  $C_V$  as a function of absolute and anharmonic characteristic temperatures. Also, we take into account the ordinary harmonic quantum effect in the procedure. Second, we derive a useful equation for the temperature dependence of  $\gamma$  as a thermodynamic identity. Combining these two concepts, we can calculate thermal pressure ( $\int \gamma C_V / V dT$ ) in  $V$ - $T$  space for almost all purposes.

In the anharmonic model presented here, the anharmonic characteristic temperature and its volume dependence are new parameters. Although our model rests on simple assumptions, the resulting EoS is consistent with experimental properties.

Lastly, we discuss the difference and advantages of our anharmonic model compared with the previous series approximation models.

### CT-EoS as experimental reference data

We calculate the CT-EoS from the ultrasonic data of Spetzler et al. (1972),  $v_i(0, 300\text{K})$ , and  $F_i(P, T)$ , in combination with  $\alpha(0, T)$  and  $C_p(0, T)$ . Before calculating the CT-EoS, we fit each experimental  $\alpha(0, T)$  and  $C_p(0, T)$  value to the empirical formula

$$M(T) = m_1 \left[ 1 + (T/m_2)^{-m_3} - m_4 \text{Exp}(T/m_5) \right]^{-m_6}, \quad (1)$$

where  $T$  is the absolute temperature. For the  $\alpha(0, T)$  curve, prior to fitting, the measurement data (Rubin et al. 1961; Yates and Panter 1962; Enck and Dommel 1965; Meincke and Graham 1965; White 1965; Leadbetter and News- ham 1969; Pathak and Vasavada 1970; Kirby et al. 1972; Rapp and Merchant 1973; Legge et al. 1979; Spinolo et al. 1979; Ming et al. 1983), e.g.,  $(dL/dT)_P / L_{293\text{K}}$ , have been corrected with the thermodynamic definition,

**Table 1**  $m_i$  of Eq. 1 for the volume thermal expansion coefficient at zero pressure,  $\alpha(0, T)$ , and the isobaric specific heat at zero pressure,  $C_p(0, T)$

$i$	$m_i$	
	$\alpha(0, T)$ in ( $K^{-1}$ )	$C_p(0, T)$ in ( $JK^{-1}mol^{-1}$ )
1	$2.49085 \times 10^{-5}$	44.4295
2	38.7213	44.0448
3	2.45015	2.00318
4	0.610481	0.0589528
5	4913.64	940.169
6	1.51746	1.99351

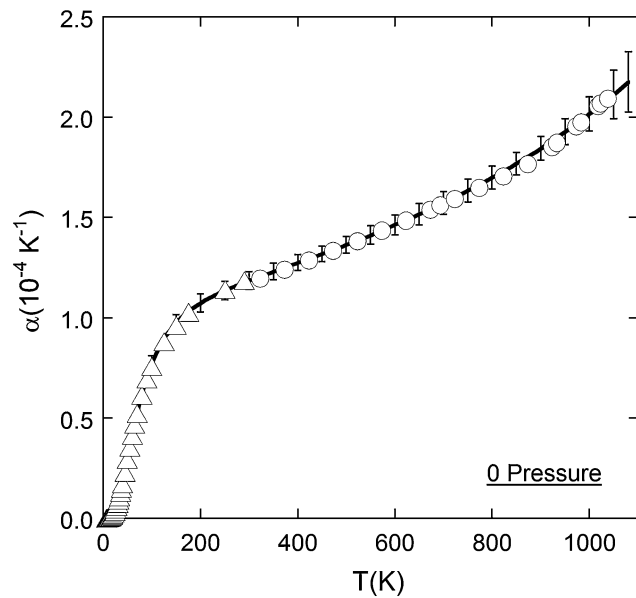


**Fig. 2** Fitting line (solid line calculated from Eq. (1) and Table 1) and experimental data (circles and triangles) for the volume thermal expansion coefficient at zero pressure. Error bars shown are 15 times greater than the errors calculated from the variance–covariance matrices ( $\epsilon_{ij}$  given in Online Resource 1). Circles Enck and Dommel (1965); triangles Meincke and Graham (1965)

$\alpha \equiv (\partial V / \partial T)_P / V$ . Fitting  $C_p(0, T)$  requires the  $C_p$  (Leadbetter and Settaree 1969) and enthalpy (Magnus 1913; Roth and Bertram 1929; Dawson et al. 1963; Holm and Grønvoold 1973; Archer 1997) data to be used simultaneously. Table 1 shows both fitting results. We give the corresponding calculated variance–covariance matrices ( $\epsilon_{ij}$ ) in Online Resource 1. Figures 2 and 3 show the fitted curves for  $\alpha(0, T)$  and  $C_p(0, T)$ , respectively, with typical experimental data (Enck and Dommel 1965; Meincke and Graham 1965; Archer 1997; Chase 1998). These figures show that Eq. 1 successfully reproduces experimental  $\alpha(0, T)$  and  $C_p(0, T)$  values with high accuracy up to the melting temperature.

Figure 4 shows the flowchart of the CT-EoS calculation, together with useful thermodynamic relations. Although

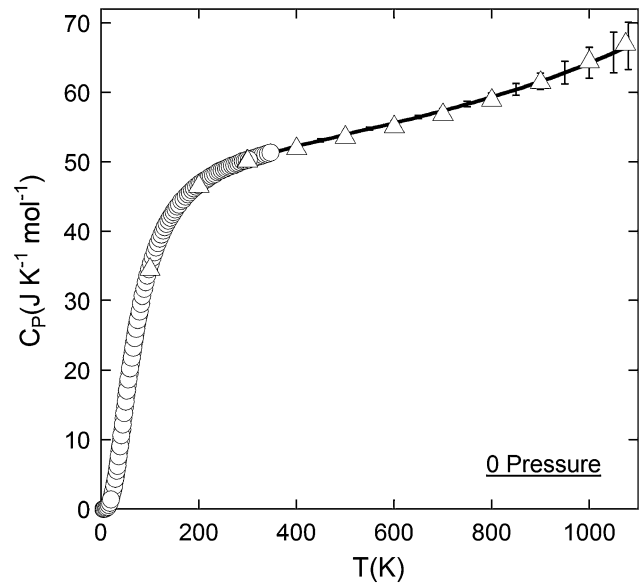


**Fig. 3** Fitting line (solid line calculated from Eq. (1) and Table 1) and experimental data (circles and triangles) for the isobaric specific heat at zero pressure. Error bars shown are 10 times greater than the errors calculated from the variance–covariance matrices ( $\epsilon_{ij}$  given in Online Resource 1). Circles Archer (1997); triangles Chase (1998)

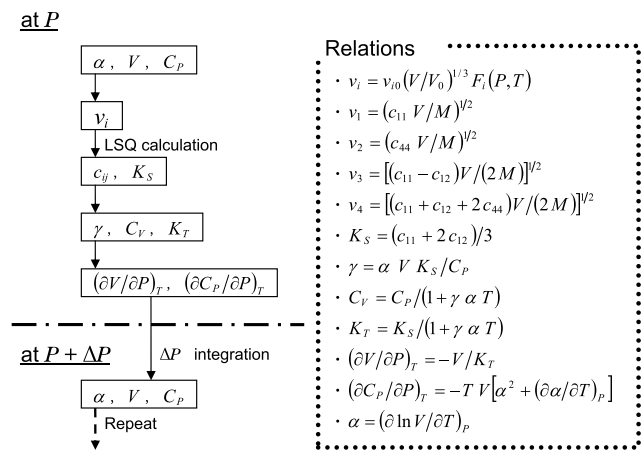


**Fig. 4** Calculation flow and relationships between sound velocities and thermodynamic properties. LSQ is the least squares method

Spetzler and Yoneda (1993) assumed an elastically isotropic material for simplicity in their test analysis, we expand our calculation to treat an elastically anisotropic cubic symmetry with three independent elastic constants ( $c_{11}$ ,  $c_{12}$ , and  $c_{44}$ ). Since Spetzler et al. (1972) have measured four individual velocities for three elastic constants, we determine the elastic constants using the least squares method (LSQ). We use the Runge–Kutta–Gill method to integrate  $(\partial V / \partial P)_T$  and  $(\partial C_p / \partial P)_T$  with respect to pressure. The pressure interval ( $\Delta P$ ) is set at 1 or 10 MPa for pressure integration; the resultant CT-EoS is not significantly

**Table 2** Molar volume,  $V$ , in the CT-EoS (this study) and estimated tolerances (in parentheses)

P/GP <sub>a</sub>	T/K					
	300	400	500	600	700	800
0	2.7016 (0.0007)	2.7350 (0.0014)	2.7713 (0.0024)	2.8107 (0.0037)	2.8537 (0.0052)	2.9007 (0.0070)
0.4	2.6583 (0.0007)	2.6882 (0.0012)	2.7206 (0.0021)	2.7554 (0.0032)	2.7929 (0.0045)	2.8335 (0.0060)
0.8	2.6188 (0.0008)	2.6460 (0.0011)	2.6751 (0.0018)	2.7063 (0.0028)	2.7397 (0.0039)	2.7755 (0.0052)

Values are in ( $10^{-5}$  m<sup>3</sup>mol<sup>-1</sup>)**Table 3** Isothermal bulk modulus,  $K_T$ , in the CT-EoS (this study) and estimated tolerances (in parentheses)

P/GP <sub>a</sub>	T/K					
	300	400	500	600	700	800
0	2.3714 (0.0151)	2.2122 (0.0150)	2.0546 (0.0160)	1.8985 (0.0188)	1.7441 (0.0215)	1.5917 (0.0222)
0.4	2.5807 (0.0159)	2.4264 (0.0157)	2.2736 (0.0165)	2.1224 (0.0190)	1.9727 (0.0218)	1.8248 (0.0232)
0.8	2.7720 (0.0166)	2.6231 (0.0164)	2.4758 (0.0169)	2.3299 (0.0190)	2.1855 (0.0219)	2.0425 (0.0239)

Values are in ( $10^{10}$  P<sub>a</sub>)**Table 4** Specific heat at constant volume,  $C_V$ , in the CT-EoS (this study) and estimated tolerances (in parentheses)

P/GP <sub>a</sub>	T/K					
	300	400	500	600	700	800
0	47.529 (0.227)	48.326 (0.280)	48.630 (0.368)	48.732 (0.477)	48.732 (0.606)	48.670 (0.824)
0.4	47.496 (0.207)	48.345 (0.261)	48.681 (0.366)	48.809 (0.479)	48.832 (0.587)	48.794 (0.765)
0.8	47.462 (0.184)	48.362 (0.241)	48.729 (0.359)	48.880 (0.481)	48.923 (0.577)	48.902 (0.718)

Values are in (JK<sup>-1</sup> mol<sup>-1</sup>)**Table 5** Grüneisen parameter,  $\gamma$ , in the CT-EoS (this study) and estimated tolerances (in parentheses)

P/GP <sub>a</sub>	T/K					
	300	400	500	600	700	800
0	1.5978 (0.0606)	1.5957 (0.0511)	1.5977 (0.0512)	1.6015 (0.0570)	1.6064 (0.0608)	1.6116 (0.0599)
0.4	1.5633 (0.0618)	1.5628 (0.0518)	1.5658 (0.0507)	1.5706 (0.0559)	1.5764 (0.0602)	1.5827 (0.0598)
0.8	1.5250 (0.0626)	1.5265 (0.0523)	1.5308 (0.0501)	1.5368 (0.0546)	1.5439 (0.0592)	1.5516 (0.0596)

Values are non-dimensional

changed by choosing different pressure intervals. Tables 2, 3, 4, and 5 show the resultant values for  $V$ ,  $K_T$ ,  $C_V$ , and  $\gamma$ , respectively. Online Resource 2 also lists the results for the other thermodynamic properties.

We have examined the CT-EoS values to identify any influences resulting from errors in the data used (Tables 2, 3, 4, 5 in parentheses). Here, likely errors include those in  $\alpha(0, T)$ ,  $C_p(0, T)$ ,  $v_i(0, 300\text{ K})$ , and  $F_i(P, T)$ . We have confirmed that the influences of other errors (e.g., lattice

constant and atomic weight) are negligible. The estimated tolerance of the experimental  $\alpha(0, T)$  values is 15 times greater than that of the error calculated from  $\varepsilon_{ij}$  (Online Resource 1) using the error propagation law (error bars in Fig. 2). We note that the total number of experimental data for  $\alpha(0, T)$  is 67 (Enck and Dommel 1965; Leadbetter and Newsham 1969; Pathak and Vasavada 1970; Kirby et al. 1972; Rapp and Merchant 1973; Spinolo et al. 1979; Ming et al. 1983) in the temperature range 300–800 K, with most

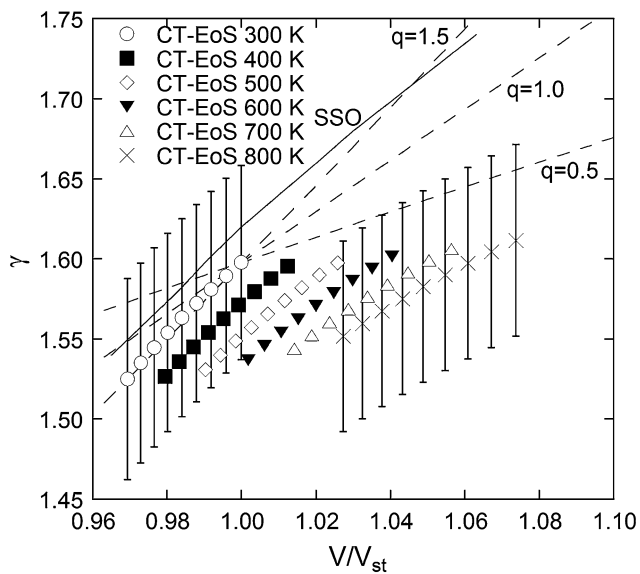


**Fig. 5** Grüneisen parameter in the CT-EoS. Error bars represent tolerances for the data at 300 and 800 K. SSO (solid line) represents the original data of Spetzler et al. (1972). Dashed lines represent ordinary power-law  $\gamma$  for  $q = 0.5, 1.0$  and  $1.5$ .  $V_{st}$  is the molar volume under the standard conditions (zero pressure and 300 K)

of these values inside the tolerance (91 % or 61 out of 67 data). Similarly, the tolerance of  $C_p(0, T)$  is estimated to be 10 times greater than the error calculated from  $\varepsilon_{ij}$  (error bars in Fig. 3). The total number of experimental  $C_p(0, T)$  and enthalpy data is 86 (Magnus 1913; Dawson et al. 1963; Leadbetter and Settaree 1969; Archer 1997) in the temperature range 300–800 K, with most of these values also inside the tolerance (84 % or 71 out of 86 data). As for the ultrasonic data of Spetzler et al. (1972), the tolerances for all  $v_i(0, 300 \text{ K})$  values are estimated equally at 7 m/s, while the tolerances of  $F_i(P, T)$  are calculated from the error matrices given by Spetzler et al. (1972). Thus, every thermodynamic parameter should be inside the estimated tolerances.

Figure 5 shows the resulting values for  $\gamma$ . The large tolerances of  $\gamma$  result almost entirely from the tolerances of  $\alpha(0, T)$ . Although we cannot completely reject the possibility of  $\gamma = \gamma(V)$ ,  $q = (\partial \ln \gamma / \partial \ln V)_T \approx 0.5$  (see dashed lines in Fig. 5) is too small compared with the other experimental estimations of 1.1–1.3 (Boehler et al. 1977; Yamamoto et al. 1987). The possibility of overestimation at low temperature and underestimation at high temperature is unlikely, because many previous studies showed nearly constant  $\gamma$  at zero pressure (e.g., Leadbetter et al. 1969; Birch 1986; Yamamoto et al. 1987; Brown 1999). The corresponding curve reported by Spetzler et al. (1972) is outside the tolerance of our calculations in the larger volume regions (see SSO in Fig. 5). This discrepancy is due to the difference in the initial condition of  $C_p(0, T)$ . Our results

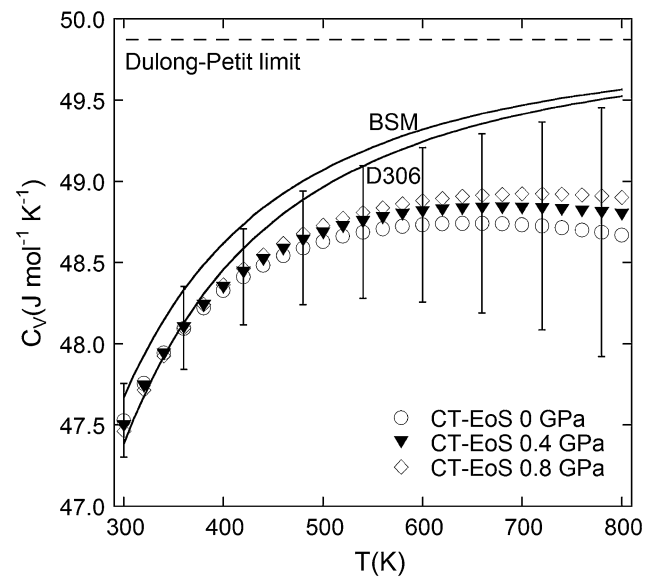


**Fig. 6** Specific heat at constant volume in the CT-EoS. Error bars represent tolerances for the data at 0 GPa. D306 (lower solid curve) and BSM (upper solid curve) are calculated using the Debye model ( $\theta_D = 306 \text{ K}$ ) and the breathing shell model (BSM) by Nüsslein and Schröder (1967), respectively. The Dulong-Petit limit (broken line) is  $49.89 \text{ JK}^{-1} \text{ mol}^{-1}$

show not only volume dependence, but also negative temperature dependence.

Figure 6 shows the resulting  $C_V$  value. The tolerances of  $\alpha(0, T)$  and  $C_p(0, T)$  constitute nearly all of the tolerance of  $C_V$  and contribute equally. At higher temperature ( $>600 \text{ K}$ ), the  $C_V(0, T)$  values are saturated and obviously smaller than the Dulong-Petit limit. The  $C_V$  value obtained from the Debye model is also shown for comparison (D306 in Fig. 6). In the Debye model, the Debye temperature ( $\theta_D$ ) is estimated from the  $v_i(0, 300 \text{ K})$  values of Spetzler et al. (1972) to be 306 K. In the higher temperature region, the  $C_V(0, T)$  value in the CT-EoS is smaller than that obtained using the Debye model beyond the tolerance. The Debye model assumes both the functional form of a lattice-vibrational spectrum (phonon spectrum) and the harmonic approximation. The inconsistency between the CT-EoS and the Debye model indicates that either (or both) of these two assumptions is (or are) unsuitable for NaCl. For a more realistic harmonic approximation model,  $C_V$  is calculated using the phonon spectrum obtained from the breathing shell model (BSM) (Nüsslein and Schröder 1967). As shown in Fig. 6, the similarity between the  $C_V$  values generated by the Debye model and the BSM implies that a difference in the phonon spectrum has little influence on the calculation of  $C_V$ . The difference in  $C_V$  between the CT-EoS and harmonic approximation models suggests that the harmonic approximation is insufficient, i.e., NaCl exhibits clear intrinsic anharmonicity. Furthermore, as shown in

Fig. 6, the pressure dependence of  $C_V$ ,  $(\partial C_V / \partial P)_T$ , in the CT-EoS is likely to have a positive sign, which is in contrast to the negative sign expected when the quasi-harmonic approximation is used.

### Anharmonic model

Recently, Cuccoli et al. (1990) and Rössler and Page (1995) investigated the  $C_V$  values for an anharmonic atomic chain. The corresponding results are qualitatively consistent with each other. Here, high-temperature behavior is characterized by the  $C_V$  values obtained from the classical anharmonic system, while low-temperature behavior is characterized by the quantum effect in the harmonic approximation. Thus, in this paper, we use a classical statistical-mechanical model for the anharmonic potential (harmonic term plus quartic term) and the quantum effect in the harmonic approximation and apply them to  $C_V$  for an anharmonic crystal. A model for the Grüneisen parameter ( $\gamma$ ) is derived from the classical anharmonic  $C_V$  model and the thermodynamic identity based on thermal pressure:

$$\left(\frac{\partial C_V}{\partial \ln V}\right)_T = C_V \left(\frac{\partial \gamma}{\partial \ln T}\right)_V + \gamma \left(\frac{\partial C_V}{\partial \ln T}\right)_V. \quad (2)$$

The Appendix gives the derivation of Eq. 2.

### Specific heat from classical statistical mechanics

Here we use classical statistical mechanics to calculate  $C_V$  for the classical anharmonic system. We assume that the  $i$ th classical vibration mode follows the potential  $E_{pi}(x_i)$  ( $x_i$  is the generalized coordinates), so that the average potential energy is given by

$$\bar{E}_{pi} = \frac{\int_{-\infty}^{\infty} E_{pi}(x_i) \exp[-E_{pi}(x_i)/(k_B T)] dx_i}{\int_{-\infty}^{\infty} \exp[-E_{pi}(x_i)/(k_B T)] dx_i}, \quad (3)$$

where  $k_B$  is Boltzmann's constant. Differentiating Eq. 3 with respect to  $T$  gives the specific heat for  $E_{pi}(x_i)$ :

$$C_{Vpi} = k_B \left( \frac{\int_{-\infty}^{\infty} E_{pi}^2(x_i) \exp[-E_{pi}(x_i)/(k_B T)] dx_i}{(k_B T)^2 \int_{-\infty}^{\infty} \exp[-E_{pi}(x_i)/(k_B T)] dx_i} - \left\{ \frac{\int_{-\infty}^{\infty} E_{pi}(x_i) \exp[-E_{pi}(x_i)/(k_B T)] dx_i}{k_B T \int_{-\infty}^{\infty} \exp[-E_{pi}(x_i)/(k_B T)] dx_i} \right\}^2 \right). \quad (4)$$

The harmonic approximation gives  $C_{Vpi} = k_B/2$ . For the positive even  $l$ th-power potential, the specific heat is  $C_{Vpi} = k_B/l$ . The specific heat of the kinetic energy for the  $i$ th mode is always given by  $k_B/2$ , which can be calculated

by substituting  $m \dot{x}_i^2/2$  and  $d\dot{x}_i$  for  $E_{pi}(x_i)$  and  $dx_i$  in Eq. 4, respectively.

During an isochoric temperature change, all average atomic positions are fixed geometrically in B1 (NaCl) structure. This is also expected in many other cubic structures (e.g. A1 (fcc), A2 (bcc), A4 (diamond), B2 (CsCl), B3 (Zincblende), etc.). On the other hand, odd terms in  $E_{pi}(x_i)$  cause the change of the average atomic position from the geometrically fixed position. Therefore, it is obvious that the fourth-order is the smallest order of anharmonic terms, and we examine the following case to calculate the anharmonic heat capacity:

$$E_{pi}(x_i) = k_i x_i^2 / 2 + s_i x_i^4 / 4 \quad (k_i > 0, s_i > 0). \quad (5)$$

Conversion from  $k_i x_i^2 / (k_B T)$  to  $x_{a_i}^2$  (i.e.,  $x_i^2 = k_B T x_{a_i}^2 / k_i$ ) gives

$$C_{Vpi-a}(\sigma_i) = k_B \left( \frac{\int_{-\infty}^{\infty} (x_{a_i}^2 / 2 + \sigma_i x_{a_i}^4 / 4) \exp[-(x_{a_i}^2 / 2 + \sigma_i x_{a_i}^4 / 4)] dx_{a_i}}{\int_{-\infty}^{\infty} \exp[-(x_{a_i}^2 / 2 + \sigma_i x_{a_i}^4 / 4)] dx_{a_i}} - \left\{ \frac{\int_{-\infty}^{\infty} (x_{a_i}^2 / 2 + \sigma_i x_{a_i}^4 / 4) \exp[-(x_{a_i}^2 / 2 + \sigma_i x_{a_i}^4 / 4)] dx_{a_i}}{\int_{-\infty}^{\infty} \exp[-(x_{a_i}^2 / 2 + \sigma_i x_{a_i}^4 / 4)] dx_{a_i}} \right\}^2 \right), \quad (6)$$

where  $\sigma_i (= s_i k_B T / k_i^2)$  is the intensity parameter of anharmonicity. Figure 7 shows the relationship between  $\sigma_i$  and  $C_{Vpi-a}$ , where  $C_{Vpi-a}$  equals  $k_B/2$  at  $\sigma_i = 0$ . For

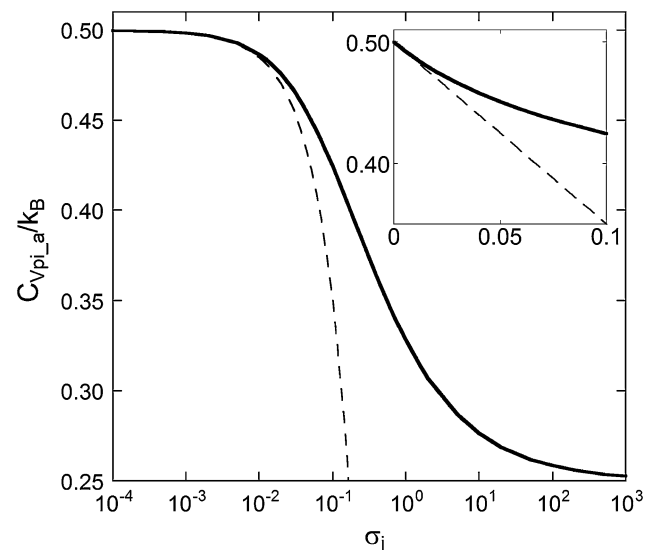


**Fig. 7** Specific heat of the potential energy for a classical anharmonic solid. Assumed potential includes positive quartic term (Eq. 5).  $\sigma_i = T/\theta_{a_i}$ . Solid lines are calculated from Eq. 6. Broken lines correspond to previous linear anharmonic model (Eqs. 17, 18). Horizontal axes of outer and inner figures are in logarithmic and linear scales, respectively

larger  $\sigma_i$  values,  $C_{V_{pi\_a}}$  approaches  $k_B/4$  as a lower limit. We define the anharmonic characteristic temperature as  $\theta_{a\_i} \equiv k_i^2 / (s_i k_B) = T / \sigma_i$ . The concept of this characteristic temperature  $\theta_{a\_i}$  is different from the anharmonicity-corrected characteristic temperature of the quasi-harmonic approximation (Holzapfel 2002; Ponkratz and Holzapfel 2004). At constant temperatures, the decrease in  $\theta_{a\_i}$  causes an increase in anharmonicity, with a subsequent decrease in  $C_{V_{pi\_a}}$ . We note that the vibration approaches a harmonic as  $\theta_{a\_i}$  increases. To ignore the mode dependence of  $\theta_{a\_i}$ , we assume a uniform energy distribution for each of the harmonic terms and the anharmonic quartic terms in  $E_{pi}(x_i)$  (Eq. 5). Consequently, we express the specific heat  $C_{Va}$  of a classical anharmonic solid as a function of  $T/\theta_a$ :

$$C_{Va} \left( \frac{T}{\theta_a} \right) = 3nN_A \left[ \frac{k_B}{2} + C_{V_{pi\_a}} \left( \frac{T}{\theta_a} \right) \right], \quad (7)$$

where  $n$  refers to the number of atoms in the chemical formula and  $N_A$  is Avogadro's number.

#### Temperature dependence of Grüneisen parameter

The temperature dependence of  $\gamma$  is related to the differential coefficients of  $C_V$  by Eq. 2. Using  $C_V = C_{Va} [T/\theta_a(V)]$  (Eq. 7) and  $\gamma_a = -(\partial \ln \theta_a / \partial \ln V)_T$ , we have

$$\left( \frac{\partial C_V}{\partial \ln V} \right)_T = \gamma_a \frac{T}{\theta_a} C'_{Va} \quad (8)$$

and

$$\left( \frac{\partial C_V}{\partial \ln T} \right)_V = \frac{T}{\theta_a} C'_{Va}. \quad (9)$$

Substituting the above two equations into Eq. 2, we have

$$\left( \frac{\partial \gamma}{\partial \ln T} \right)_V = (\gamma_a - \gamma) \frac{T}{\theta_a} \frac{C'_{Va}}{C_{Va}}. \quad (10)$$

Assuming  $\theta_a$  is a function of only  $V$ ,  $\gamma_a$  is constant or independent of  $T$  at a given  $V$ . Equation 10 can be solved analytically to obtain

$$\gamma(T) = \gamma_a + \frac{3nR(\gamma_h - \gamma_a)}{C_{Va}(T/\theta_a)}, \quad (11)$$

where  $\gamma_h = \gamma(V, 0 \text{ K})$  is the harmonic Grüneisen parameter and  $R$  is the gas constant. Incidentally, Eq. 11 is equivalent to Eq. (2.3) in Leadbetter (1968),  $\gamma C_V = \gamma^{qh} C_V^{qh} + \gamma^{anh} \Delta C_V^{anh}$ .

#### Modeling of thermal pressure

We use Eq. 11 to model  $\gamma$  as a function of  $V$  and  $T$ . For simplicity, in the case of NaCl, we assume a constant  $\gamma_a$  regardless of  $V$  and an ordinary power-law volume-dependent  $\gamma_h$ . Hence,

$$\gamma(V, T) = \gamma_a + 6R \frac{\gamma_h(V) - \gamma_a}{C_{Va} [T/\theta_a(V)]} \quad (12)$$

with

$$\gamma_h(V) = \gamma_{h\_st} (V/V_{st})^{q_h}, \quad (13)$$

and

$$\theta_a(V) = \theta_{a\_st} (V/V_{st})^{-\gamma_a}, \quad (14)$$

where the subscript “st” refers to the standard conditions (zero pressure and 300 K). We confirm the validity of this simplification later by comparing this anharmonic model with the CT-EoS.

Here, we write the molar volume at 0 K and zero pressure as  $V_0$ . We model the specific heat  $C_V(V_0, T)$  as the product of  $C_{Va}(T/\theta_a)$  (Eq. 7) and the quasi-harmonic quantum correction,

$$C_V(V_0, T) = C_{Va} \left[ \frac{T}{\theta_a(V_0)} \right] \frac{1}{6N_A} \int_0^{\omega_{Max}} \frac{[\hbar\omega / (k_B T)]^2 \exp [\hbar\omega / (k_B T)]}{(\exp [\hbar\omega / (k_B T)] - 1)^2} g(\omega) d\omega, \quad (15)$$

where  $\omega$  is the angular frequency,  $\hbar$  is Planck's constant divided by  $2\pi$ , and  $g(\omega)$  is the frequency distribution function from BSM (Nüsslein and Schröder 1967).

Using the models for  $\gamma(V, T)$  (Eqs. 12, 13, 14) and  $C_V(V_0, T)$  (Eq. 15),  $C_V(V, T)$  can be derived by integrating Eq. 2 with respect to  $\ln V$ . Hence, we obtain the thermal pressure ( $\int_0^T \gamma C_V V^{-1} dT$ ) as a function of  $V$  and  $T$ . Additional knowledge of the compression curve, e.g., the Birch-Murnaghan EoS (Murnaghan 1944; Birch 1952), Vinet EoS (Vinet et al. 1987), or pseudospinodal EoS (Baonza et al. 1995; Taravillo et al. 2002), at a certain temperature (e.g. 300 K) complements the total EoS.

#### Comparing with the CT-EoS

We use the CT-EoS results to execute the LSQ calculation for the anharmonic model using the CT-EoS results (Tables 2, 3, 4, 5). The resultant model parameters are  $\gamma_{h\_st} = 1.622 \pm 0.025$ ,  $q_h = 1.35 \pm 0.57$ ,  $\theta_{a\_st} = (86 \pm 12) \times 10^3 \text{ K}$ , and  $\gamma_a = 9.5 \pm 3.3$ . Figure 8 compares the  $\gamma$  values obtained from the anharmonic model and the CT-EoS. Here, both the temperature and volume dependences of the anharmonic model are consistent with those of the CT-EoS, within an allowable tolerance, so that our anharmonic model is more desirable than the frequently used  $\gamma = \gamma(V)$  model. Figure 9 compares the  $C_V$  value of the anharmonic model with that of the CT-EoS. Though the volume changes in  $C_V$  have to be computed by

integrating Eq. 2 using the models of  $\gamma(V, T)$  and  $C_V(V_0, T)$ ,  $C_V$  in this study is easily calculated from Eq. 15, in which  $V$  is substituted for  $V_0$  and

$$g(V, \omega) = \exp \left\{ \frac{\gamma_h}{q} \left[ \left( \frac{V}{V_{st}} \right)^q - \left( \frac{V_0}{V_{st}} \right)^q \right] \right\} \\ g \left( \omega / \exp \left\{ \frac{\gamma_h}{q} \left[ \left( \frac{V_0}{V_{st}} \right)^q - \left( \frac{V}{V_{st}} \right)^q \right] \right\} \right) \quad (16)$$

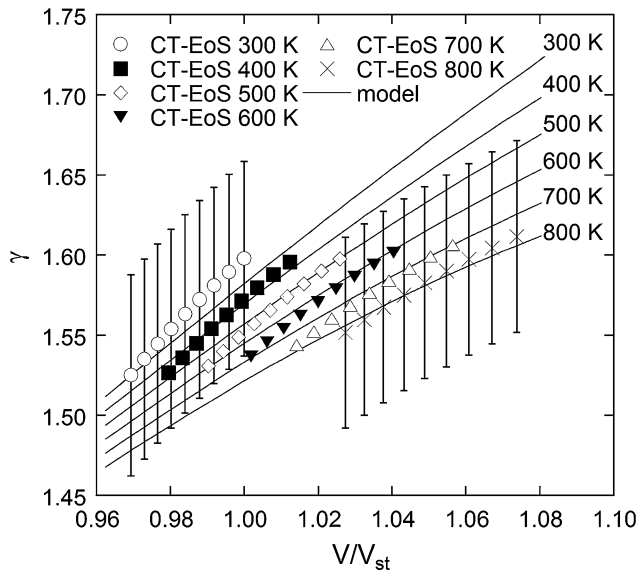


**Fig. 8** Grüneisen parameter calculated using the anharmonic model (solid lines). The CT-EoS data used are the same as those in Fig. 5

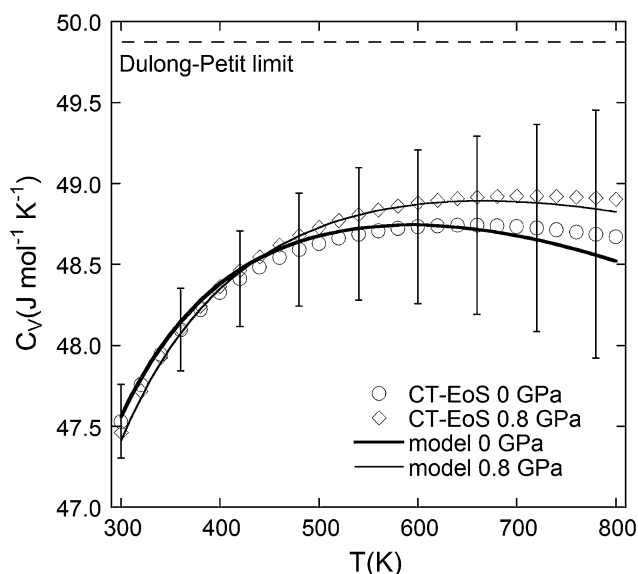


**Fig. 9** Specific heat calculated using the anharmonic model (bold line 0 GPa, thin line 0.8 GPa). The CT-EoS data used are the same as those in Fig. 6

is substituted for  $g(\omega)$ . In this calculation, we use the data for  $V$  in Table 2. The calculated  $C_V$  value is consistent with that of the CT-EoS, within an allowable tolerance. These results demonstrate that our modeling and parameterization are sufficient.

## Discussion

Our recalculation of the CT-EoS using correct  $C_P$  data (Eq. 1 with Table 1; Fig. 3) yields very different  $\gamma$  values from those of Spetzler et al. (1972) (Fig. 5). The error estimation shown in Tables 2, 3, 4, and 5 shows that our CT-EoS achieves a level of accuracy that has not been achieved before. The new CT-EoS is important as a highly accurate experimental reference for physical modeling of thermoelasticity of solids. Boehler (1981) directly measured  $(\partial T / \partial P)_S$  for the NaCl-B1 phase up to 5 GPa and 1,073 K. Because  $(\partial T / \partial P)_S = \gamma T / K_S$ , we can compare the results with that of the CT-EoS. Figure 10 shows excellent agreement between the measured  $(\partial T / \partial P)_S$  and  $\gamma T / K_S$  from the present CT-EoS at 298, 473, 673, and 800 K, which supports the reliability of the present CT-EoS.

The  $K_T$ - $V$  relationship (Fig. 11) is one of the most useful properties of the CT-EoS, where the temperature dependency of  $K_T$  is essentially negligible (Birch 1986; Anderson 1999). However, extrapolation of the  $K_T = K_T(V)$  hypothesis requires more detailed consideration. To confirm that  $K_T = K_T(V)$ , we examine the CT-EoS to determine whether  $(\partial \ln K_T / \partial \ln V)_T = (\partial \ln K_T / \partial \ln V)_P$  is satisfied; that is,

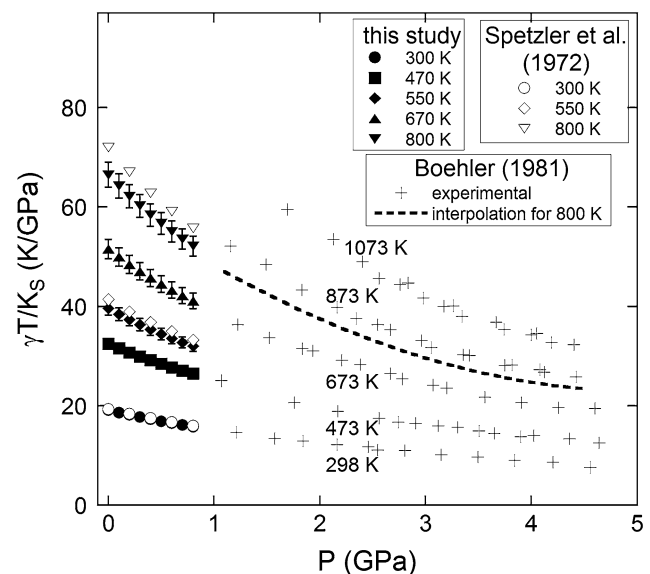


**Fig. 10** Comparison of the adiabat data  $((\partial T / \partial P)_S = \gamma T / K_S)$ . The data sources are specified in the legend inside the plot. The broken line shows the line at 800 K interpolated from the original data of Boehler (1981)



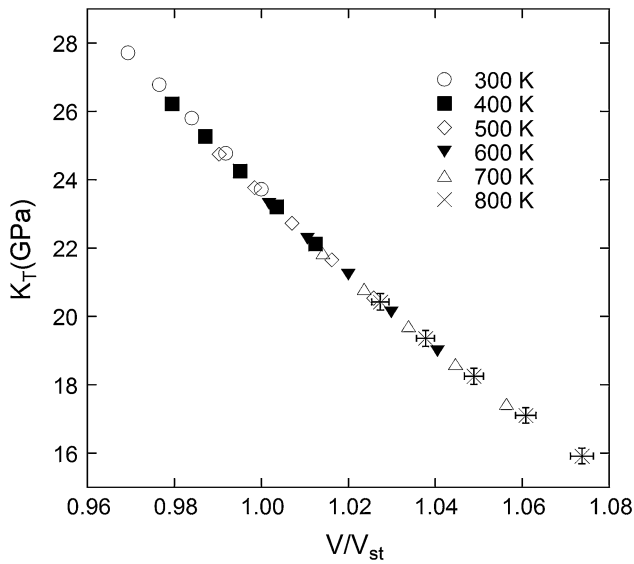


**Fig. 11** Isothermal bulk modulus in the CT-EoS. Error bars represent tolerances for the data at 800 K

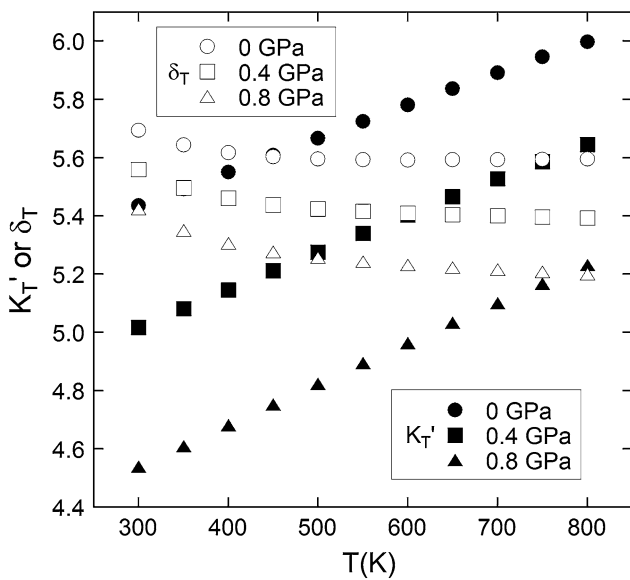


**Fig. 12** Pressure derivative of the isothermal bulk modulus ( $K'_T$ ) and the isothermal Anderson-Grüneisen parameter ( $\delta_T$ ) in the CT-EoS

$K'_T = \delta_T$  ( $K'_T$  being the pressure derivative of  $K_T$ , and  $\delta_T$  the isothermal Anderson-Grüneisen parameter). However, the results in Fig. 12 indicate that the CT-EoS does not satisfy  $K'_T = \delta_T$ . Thus,  $K_T = K_T(V)$  only holds within a limited  $P$ – $T$  range, so that an EoS based on this hypothesis cannot be supported.

To evaluate  $C_V$  for positive quartic anharmonicity (Eq. 5), we use statistical mechanics, which enables us to avoid the imperfection of series approximation. The lowest order series approximation

**Table 6** Specific heat of a classical positive quartic anharmonic solid ( $C_{V_a}/3nR-1$ )

$T/\theta_a$	$\times 10^{-4}$	$\times 10^{-3}$	$\times 10^{-2}$
1.0	−0.000150 (99.88)	−0.001482 (98.82)	−0.013448 (89.65)
1.2	−0.000180 (99.85)	−0.001775 (98.59)	−0.015822 (87.90)
1.4	−0.000210 (99.83)	−0.002066 (98.36)	−0.018110 (86.24)
1.7	−0.000254 (99.79)	−0.002499 (98.02)	−0.021392 (83.89)
2.0	−0.000299 (99.76)	−0.002930 (97.68)	−0.024509 (81.7)
2.5	−0.000374 (99.70)	−0.003642 (97.12)	−0.029377 (78.34)
3.2	−0.000478 (99.62)	−0.004625 (96.35)	−0.035602 (74.17)
4.0	−0.000597 (99.52)	−0.005730 (95.49)	−0.042010 (70.02)
5.0	−0.000746 (99.40)	−0.007084 (94.45)	−0.049156 (65.54)
6.2	−0.000923 (99.26)	−0.008671 (93.24)	−0.056715 (60.98)
8.0	−0.001189 (99.05)	−0.010979 (91.49)	−0.066446 (55.37)

Values are non-dimensional. Values in parentheses are ratios (in %) to the linear anharmonic model (Eqs. 17, 18)

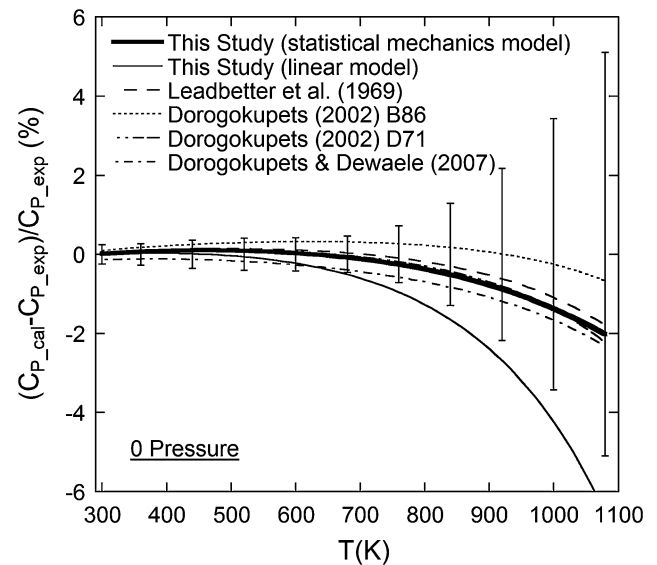


**Fig. 13** Comparison of the isobaric specific heat at zero pressure. The relative ratios of model values to experimental values are shown. Experimental values are from Eq. 1 with Table 1. Bold line statistical-mechanical model from Eqs. 6 and 7; thin lines linear anharmonicity models from Eqs. 17 and 18. Parameters used are listed in Table 7. Error bars are shown for experimental values

**Table 7** Parameters for the Grüneisen parameter,  $\gamma$ . Previous data are converted according to the definition of this study. Values in parentheses are for  $V_{st}$

Parameter	This Study	Leadbetter et al. (1969)	Dorogokupets (2002)		Dorogokupets & Dewaele (2007)
			B86	D71	
$\gamma_{h_{st}}$	1.622	1.622	1.608	1.657	1.64
$q_h$	1.35	1.10	(1.034)	(1.532)	(1.382)
$\theta_{a_{st}}$ ( $10^3$ K)	86	84.5	105.0	73.1	62.4
$\gamma_a$	9.5	7	7.348	8.435	7.02

$$C_{Va}/(3nR) = 1 + AT \quad (17)$$

is the most often used at the moment. Also, for NaCl, some researchers (Leadbetter et al. 1969; Dorogokupets 2002; Dorogokupets and Dewaele 2007) have proposed EoSs based on Eq. 17. The anharmonic parameter  $A$  is related to  $\theta_a$  in the low-temperature approximation (Kittel 1953; Oganov and Dorogokupets 2004):

$$A = -3/(2\theta_a). \quad (18)$$

As shown in Table 6 and Fig. 7, the linear approximation Eq. 17 is good for  $T/\theta_a < 2 \times 10^{-3}$ , but inadequate for  $T/\theta_a > 10^{-2}$ . For NaCl at zero pressure, the condition  $T/\theta_a > 10^{-2}$  is matched at above 600 K.

If our anharmonic model includes sufficient physical basis, thermoelastic properties should be estimated accurately even beyond the  $P$ – $T$  conditions in which the CT-EoS data are used for parameter optimization. Figure 13 compares experimental  $C_p$  at zero pressure with the present and previous anharmonic models (Leadbetter et al. 1969; Dorogokupets 2002; Dorogokupets and Dewaele 2007). In the anharmonic models, the values of  $C_p$  are calculated from  $C_p = C_V(1 + \gamma \alpha T)$  with the values of  $\alpha(0, T)$  from Eq. 1 and Table 1. Table 7 lists the parameters for the anharmonic models. Figure 13 shows that our model succeeds in estimating  $C_p$  with high accuracy even beyond 800 K, which is the high-temperature limit of the CT-EoS data. However, previous linear anharmonic models can also reproduce experimental  $C_p$  with equally high accuracy. The linear anharmonic model (Eqs. 17, 18) with parameters in this study underestimates the value of  $C_p$  above 600 K, because the condition  $T/\theta_a > 10^{-2}$  is appropriate. Conversely, all previous models use small values of  $\gamma_a$  (Table 7) to avoid underestimating  $C_p$  at high temperatures. Equation 11 can be rewritten as

$$\gamma = (3nR\gamma_h + \Delta C_{Va} \gamma_a)/C_{Va} \quad (19)$$

with  $\Delta C_{Va} = C_{Va} - 3nR$ . Because the sign of  $\Delta C_{Va}$  is always negative for positive quartic anharmonicity, Eq. 19 implies that a small value of  $\gamma_a$  causes overestimation of  $\gamma$  at high temperatures. Figure 14 compares experimental  $\gamma$  at zero pressure to the present and previous anharmonic models (Leadbetter et al. 1969; Dorogokupets 2002; Dorogokupets and Dewaele 2007). Our model best reproduces

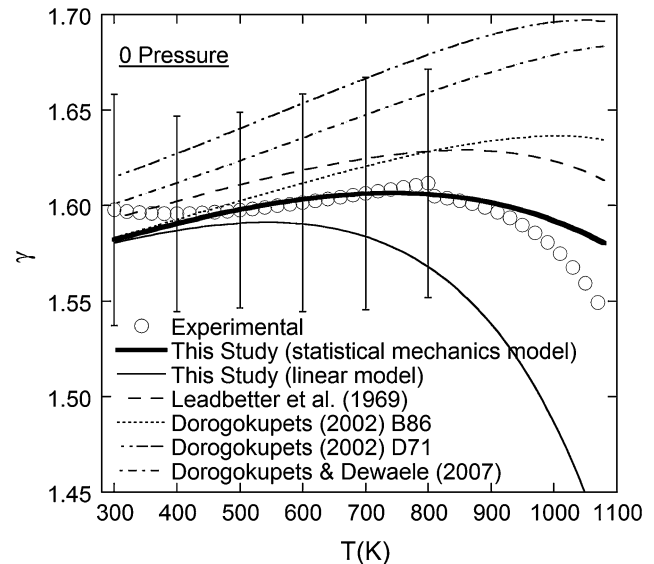


**Fig. 14** Comparison of the Grüneisen parameter at zero pressure. Experimental values up to 800 K are from the CT-EoS results, and for over 800 K are calculated from  $\alpha$ ,  $C_p$  (Eq. 1 with Table 1) and  $K_S$  (Slagle and McKinstry 1967). Bold line statistical-mechanical model from Eqs. 6, 7, and 12; thin lines linear anharmonicity models from Eqs. 12, 17, and 18. Parameters used are listed in Table 7. Error bars are shown for the CT-EoS results

the experimental values. All previous models overestimate  $\gamma$ , however, within the margin of error.

The good agreement between our anharmonic model and the experimental  $C_p$  (Fig. 13),  $C_V$  (Fig. 9) and  $\gamma$  (Figs. 8, 14) shows the validity of our anharmonic model for the NaCl-B1 phase below 1 GPa. Since  $\theta_a$  depends on  $V$  for large powers of  $\gamma_a$  (e.g., 9.5 in this study) in Eq. 14, a slight decrease in  $V$  causes a rapid increase in  $\theta_a$  so that the anharmonicity disappears. For example,  $\theta_a$  is nearly  $1 \times 10^6$  K at  $V/V_{st} \approx 0.8$  (about 10 GPa), and therefore, 1,000 K gives  $T/\theta_a \approx 10^{-3}$ , at which a quasi-harmonic approximation almost holds (Table 6; Fig. 7).

The positive quartic anharmonicity reduces both  $C_V$  and  $\gamma$  values, especially at low pressure. Therefore, previous quasi-harmonic models with the power-law  $\gamma$  have overestimated thermal pressure at zero pressure. Consequently,  $\alpha(0, T)$  values have also been overestimated, as recognized in Decker's (1971) EoS. To reproduce  $\alpha(0, T)$  values,

Brown (1999) assumed that  $\gamma$  values are constant regardless of  $V$  in the expanded volume region. The present CT-EoS and anharmonic model give nearly constant  $\gamma$  values regardless of  $V$  at zero pressure (Table 5 and Fig. 14). Thus, the anharmonic model supports Brown's (1999) hypothesis for  $\gamma$  only at zero pressure.

In the preceding section, we simply calculated  $C_V$  from Eqs. 15 and 16 to avoid numerical integration of Eq. 2. This procedure causes overestimation of  $(\partial C_V / \partial \ln V)_T$ . Using Eqs. 17 and 18 and the Debye heat capacity  $C_{V,D}$ , we can write the overestimation as

$$\delta(\partial C_V / \partial \ln V)_T = \frac{3T^2}{2\theta_D\theta_a}(\gamma_a - \gamma_h)C'_{V,D}. \quad (20)$$

Because the maximum value of  $C'_{V,D}$  is  $3.168(3nR)$  at  $T = 0.164 \theta_D$ , the maximum error in  $(\partial C_V / \partial \ln V)_T$  is  $0.128(\gamma_a - \gamma_h)(3nR)(\theta_D / \theta_a)$ . For the compression from  $V_{st}$  to  $0.9V_{st}$  in the NaCl case, this procedural error is less than 0.3 % of  $C_V$  and negligible.

Anharmonicity is known to cause frequency shifts in vibration modes, where these frequency shifts typically influence the quantum effect of  $C_V$  (Schwarz 1976). Here we estimate the frequency shift in a one-particle model to roughly ascertain the magnitude of the influence. At sufficiently high temperatures ( $T / \theta_a \approx 10^{-1}$ ), the frequency is calculated to shift just 3.5 % to a higher frequency. This amount is comparable to the error in the frequency distribution function and can therefore be ignored. Schwarz (1976) rigorously calculated the value of  $C_V$  for an anharmonic oscillator with harmonic and positive quartic potential. The result (see Fig. 1 in Schwarz 1976) shows that the harmonic quantum correction is satisfactory even under a weak anharmonic condition,  $\lambda \leq 0.05$  ( $\lambda = \theta_E / (4\theta_a)$ , where  $\theta_E$  is the Einstein characteristic temperature). Thus, our model works well under the condition  $\theta_E \leq \theta_a / 5$ . Note that our NaCl analysis satisfies the condition (maximum  $\theta_E \approx \theta_D = 306\text{K}$  and  $\theta_a > 40 \times 10^3\text{K}$ ).

There are two bold assumptions in our anharmonic model. The first of these is uniform  $\theta_a$  regardless of vibration mode. The second is constant  $\gamma_a$  regardless of  $V$ . The large errors in  $C_V$  and  $\gamma$  (Tables 4, 5; Figs. 8, 9) make it difficult to verify our assumptions. For a stricter formulation and its evaluation, we need a precise measurement for thermal expansion ( $\alpha$ ), heat capacity ( $C_P$  or  $C_V$ ), and vibrational spectrum ( $g(\omega)$ ), especially at high temperatures. Also, high-pressure measurements (e.g. Murphy et al. 2011; Yoneda et al. 2009) are important. Very recently, Matsui et al. (2012) reported the simultaneous measurements of ultrasonic velocities and lattice constants of the polycrystalline NaCl-B1 phase up to 12 GPa and 673 K. Extending the  $P$ - $T$  range of the CT-EoS to study intrinsic anharmonicity would require a similar experiment at higher temperatures with a narrower  $P$ - $T$  interval.

For a complicated crystal structure, average atomic positions may be affected by temperature change even under the isochoric condition. In this case, the odd term in  $E_{pi}(x_i)$  is not negligible. Even in the 3rd-order anharmonicity of  $E_{pi}(x_i)$ , Eq. 17 is applicable as a low-temperature approximation (Kittel 1953). However, it is uncertain what the advantage of Eq. 6 as a substitute for Eq. 17 is at high temperature.

In KCl and KBr case, anharmonicity causes the heat capacity  $C_V$  to exceed the Dulong-Petit limit (Leadbetter et al. 1969). This means that the sign of  $A$  in Eq. 17 is positive; conversely,  $\theta_a$  is negative from Eq. 18. For negative  $\theta_a$ , the potential  $E_{pi}$  shows negative divergence; therefore, the potential heat capacity Eq. 4 cannot be integrated without adding a positive even higher-order term. For the positive 6th-order term, we obtain

$$E_{pi}(x_i) = k_i \frac{x_i^2}{2} + s_i \frac{x_i^4}{4} + t_i \frac{x_i^6}{6} \quad (k_i > 0, s_i < 0, t_i > 0). \quad (21)$$

Equation 4 with Eq. 21 can be calculated by introducing the 6th-order anharmonic characteristic temperature  $\theta_{a,6} \equiv (k_i^3 / (t_i k_B^2))^{1/2}$ . However, it is empirical and preliminary. The relation  $\theta_{a,6} = -2.212\theta_a$  seems to match the temperature dependence of  $C_V$  for both KCl and KBr simultaneously (Fig. 15). Although the potential (Eq. 21) with  $\theta_{a,6} = -2.212\theta_a$  is obviously a triple-well potential, we cannot ascertain its physical meaning or generality at present. Thus, further study is needed for the negative  $\theta_a$  case.

## Conclusion

Recalculating the complete travel-time equation of state (CT-EoS) of the NaCl (B1 phase) for temperature up to 800 K and pressure up to 0.8 GPa gives a highly accurate experimental reference for physical modeling of thermoelastic properties of solids. The CT-EoS yields accurate  $\gamma$  and  $C_V$  values that cannot be obtained by either the ordinary quasi-harmonic Debye or the  $\gamma = \gamma(V)$  models. Carefully comparing the  $C_V$  values of the harmonic models and CT-EoS shows that NaCl has clear intrinsic anharmonicity.

We introduced positive quartic anharmonicity to explain the temperature and pressure dependences of  $\gamma$  and  $C_V$  in the CT-EoS. Here, we used classical statistical mechanics for the anharmonic potential and quantum effects in a harmonic approximation and applied them to the  $C_V$  model of an anharmonic crystal (Eqs. 6, 7, 15). We devised a temperature-dependent model of  $\gamma$  (Eq. 11) from the thermodynamic identity (Eq. 2). The anharmonic model with only two additional parameters ( $\theta_a$  and  $\gamma_a$ ) can reasonably reproduce the properties of  $\gamma$  and  $C_V$  simultaneously in the CT-EoS. We examined the applicability limit of the previous linear anharmonic model (Eq. 17), and at high temperatures

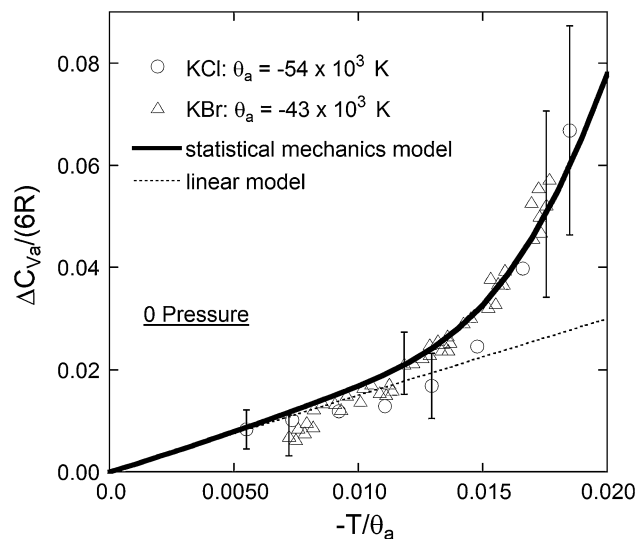


**Fig. 15** Intrinsic anharmonic contributions to the specific heat at constant volume for KCl and KBr. Experimental data and the anharmonic characteristic temperatures  $\theta_a$  are from Leadbetter et al. (1969). The statistical mechanics model (*bold line*) is calculated from Eqs. 4 and 21 with the condition  $\theta_{a,6} = -2.212\theta_a$ . The linear model (*dotted line*) is from Eqs. 17 and 18. Error bars are shown for experimental data

( $T/\theta_a > 10^{-2}$ ), the linear model optimized with respect to heat capacities ( $C_V$  or  $C_P$ ) overestimates  $\gamma$ .

**Acknowledgments** We are grateful to Dr. Peter I. Dorogokupets, Dr. Koji Masuda, and Dr. Katsuhiko Tsukimura for their constructive comments and to an anonymous reviewer for comments about the systematic error of the CT-EoS analyses. This paper presents results from a joint research program carried out at the Institute for Study of the Earth's Interior, Okayama University.

**Open Access** This article is distributed under the terms of the Creative Commons Attribution License which permits any use, distribution, and reproduction in any medium, provided the original author(s) and the source are credited.

## Appendix

$$\text{Derivation of } \left(\frac{\partial C_V}{\partial \ln V}\right)_T = C_V \left(\frac{\partial \gamma}{\partial \ln T}\right)_V + \gamma \left(\frac{\partial C_V}{\partial \ln T}\right)_V$$

The relationship between the internal energy ( $U$ ) and the Helmholtz free energy ( $F$ ) is

$$F = U - TS, \quad (22)$$

where  $S$  is entropy. Specific heat and pressure can be defined as partial derivatives of the energy:

$$C_V = \left(\frac{\partial U}{\partial T}\right)_V, \quad (23)$$

$$P = -\left(\frac{\partial F}{\partial V}\right)_T. \quad (24)$$

Maxwell's thermal pressure relation is

$$\left(\frac{\partial S}{\partial V}\right)_T = \left(\frac{\partial P}{\partial T}\right)_V = \gamma C_V / V. \quad (25)$$

Using the above equations, we obtain the volume derivative of the specific heat as

$$\left(\frac{\partial C_V}{\partial V}\right)_T = \left(\frac{\partial U}{\partial T \partial V}\right) = \left(\frac{\partial (F + TS)}{\partial V \partial T}\right) \quad (26a)$$

$$= -\left(\frac{\partial P}{\partial T}\right)_V + \left(\frac{\partial (S + T(\partial S / \partial T)_V)}{\partial V}\right)_T \quad (26b)$$

$$= -\frac{\gamma}{V} C_V + \frac{\gamma}{V} C_V + \left(\frac{\partial^2 S}{\partial V \partial \ln T}\right) \quad (26c)$$

$$= \left(\frac{\partial (\gamma C_V / V)}{\partial \ln T}\right)_V \quad (26d)$$

$$= \frac{1}{V} \left( C_V \left(\frac{\partial \gamma}{\partial \ln T}\right)_V + \gamma \left(\frac{\partial C_V}{\partial \ln T}\right)_V \right). \quad (26e)$$

Thus, we have

$$\left(\frac{\partial C_V}{\partial \ln V}\right)_T = C_V \left(\frac{\partial \gamma}{\partial \ln T}\right)_V + \gamma \left(\frac{\partial C_V}{\partial \ln T}\right)_V. \quad (27)$$

## References

- Anderson OL (1999) The volume dependence of thermal pressure in perovskite and other minerals. *Phys Earth Planet Int* 112: 267–283
- Archer DG (1997) Enthalpy Increment Measurement for NaCl(cr) and KBr(cr) from 4.5 K to 350 K. Thermodynamic properties of the NaCl + H<sub>2</sub>O system. 3. *J Chem Eng Data* 42:281–292
- Baonza VG, Cáceres M, Núñez J (1995) Universal compressibility behavior of dense phases. *Phys Rev B* 51:28–37
- Birch F (1952) Elasticity and constitution of the Earth's interior. *J Geophys Res* 57:227–286
- Birch F (1986) Equation of state and thermodynamic parameters of NaCl to 300 kbar in the high-temperature domain. *J Geophys Res* 91:4949–4954
- Boehler R (1981) Adiabats ( $\partial T / \partial P$ )<sub>S</sub> and Grüneisen parameter of NaCl up to 50 kilobars and 800°C. *J Geophys Res* 86:7159–7162
- Boehler R, Getting IC, Kennedy GC (1977) Grüneisen parameter of NaCl at high compressions. *J Phys Chem Solids* 38:233–236
- Brown JM (1999) The NaCl pressure standard. *J Appl Phys* 86:5801–5808
- Chase MW (1998) NIST-JANAF Thermochemical Tables. Part I, 4th edn. AIP, New York
- Cowley ER (1971) Anharmonic contributions to the thermodynamic properties of sodium chloride. *J Phys C Solid State Phys* 4:988–997
- Cuccoli A, Tognetti V, Vaia R (1990) Thermodynamic properties of a quantum chain with nearest-neighbor anharmonic interactions. *Phys Rev B* 41:R9588–R9591

- Dawson R, Brackett EB, Brackett TE (1963) A high temperature calorimeter; the enthalpies of  $\alpha$ -aluminum oxide and sodium chloride. *J Phys Chem* 67:1669–1671
- Decker DL (1971) High-pressure equation of state for NaCl, KCl, and CsCl. *J Appl Phys* 42:3239–3244
- Dorogokupets PI (2002) Critical analysis of equations of state for NaCl. *Geochem Inter* 40(Supplement 1):S132–S144
- Dorogokupets PI, Dewaele A (2007) Equations of state of MgO, Au, Pt, NaCl-B1, and NaCl-B2: internally consistent high-temperature pressure scales. *High Press Res* 27:431–446. doi:10.1080/08957950701659700
- Enck FD, Dommel JG (1965) Behavior of the thermal expansion of NaCl at elevated temperatures. *J Appl Phys* 36:839–844
- Holm BJ, Grønvdal F (1973) Enthalpies of fusion of the alkali cryolites determined by drop calorimetry. *Acta Chem Scand* 27:2043–2050
- Holzappel WB (2002) Anharmonicity in the equations of state of Cu, Ag, and Au and related uncertainties in the realization of a practical pressure scale. *J Phys Condens Matter* 14:10525–10531
- Kirby RK, Hahn TA, Rothrock BD (1972) Thermal expansion. In: Gray DE (ed) *American institute of physics handbook*, 3rd edn. McGraw-Hill, New York, pp 4-119–4-142
- Kittel C (1953) *Introduction to solid state physics*. Wiley, New York
- Leadbetter AJ (1968) Anharmonic effects in the thermodynamic properties of solids II. Analysis of data for lead and aluminium. *J Phys C Solid State Phys* 1:1489–1504
- Leadbetter AJ, Newsham DMT (1969) Anharmonic effects in the thermodynamic properties of solids III. A liquid gallium immersion dilatometer for the range 50–700°C: thermal expansivities of Hg, Ga, NaCl and KCl. *J Phys C Solid State Phys* 2:210–219
- Leadbetter AJ, Settaree GR (1969) Anharmonic effects in the thermodynamic properties of solids IV. The heat capacities of NaCl, KCl and KBr between 30 and 500°C. *J Phys C Solid State Phys* 2:385–392
- Leadbetter AJ, Newsham DMT, Settaree GR (1969) Anharmonic effects in the thermodynamic properties of solids V. Analysis of data for NaCl, KCl and KBr. *J Phys C Solid State Phys* 2:393–403
- Legge JC, Robinson MC, Shapiro MM (1979) Capacitance determination of the area thermal expansion of dielectric crystals. *Rev Sci Instrum* 50:832–834
- Magnus A (1913) Specific heat measurements of stable solids at high temperatures. *Phys Z* 14:5–11 (in German)
- Matsui M, Higo Y, Okamoto Y, Irifune T, Funakoshi K (2012) Simultaneous sound velocity and density measurements of NaCl at high temperatures and pressures: application as a primary pressure standard. *Am Mineral* 97:1670–1675. doi:10.2138/am.2012.4136
- Meincke PPM, Graham GM (1965) The thermal expansion of alkali halides. *Can J Phys* 43:1853–1866
- Ming LC, Manghnani MH, Balogh J, Qadri SB, Skelton EF, Jamieson JC (1983) Gold as a reliable internal pressure calibrant at high temperature. *J Appl Phys* 54:4390–4397
- Murnaghan FD (1944) The compressibility of media under extreme pressures. *Proc Nat Acad Sci USA* 30:244–247
- Murphy CA, Jackson JM, Sturhahn W, Chen B (2011) Grüneisen parameter of hcp-Fe to 171 GPa. *Geophys Res Lett* 38:L24306. doi:10.1029/2011GL049531
- Nüsslein V, Schröder U (1967) Calculations of dispersion curves and specific heat for LiF and NaCl using the breathing shell model. *Phys Status Solidi* 21:309–314
- Oganov AR, Dorogokupets PI (2003) All-electron and pseudopotential study of MgO: equation of state, anharmonicity, and stability. *Phys Rev B* 67:224110/1–224110/11. doi:10.1103/PhysRevB.67.224110
- Oganov AR, Dorogokupets PI (2004) Intrinsic anharmonicity in equations of state and thermodynamics of solids. *J Phys Condens Matter* 16:1351–1360. doi:10.1088/0953-8984/16/8/018
- Pathak PD, Vasavada NG (1970) Thermal expansion of NaCl, KCl and CsBr by X-ray diffraction and the law of corresponding states. *Acta Crystallogr Sect A* 26:655–658
- Ponkratzen U, Holzappel WB (2004) Equations of state for wide ranges in pressure and temperature. *J Phys Condens Mat* 16:S963–S972. doi:10.1088/0953-8984/16/14/005
- Powell DGM, Fletcher GC (1965) Thermal expansion and other properties of sodium chloride. *Aust J Phys* 18:205–217
- Rapp JE, Merchant HD (1973) Thermal expansion of alkali halides from 70 to 570 K. *J Appl Phys* 44:3919–3923
- Rössler T, Page JB (1995) Quantum mechanics, quantum-classical correspondence, thermodynamics, and response of a small anharmonic periodic chain. *Phys Rev B* 51:11382–11392
- Roth WA, Bertram W (1929) Measurements of the specific heat of metallurgically important substances in a large temperature interval with help of two new calorimeter types. *Z Elektrochem* 35:297–308 (in German)
- Rubin T, Johnston HL, Altman HW (1961) Thermal expansion of rock salt. *J Phys Chem* 65:65–68
- Schwarz M Jr (1976) Statistical thermodynamics of an anharmonic oscillator. *J Stat Phys* 15:255–261
- Slagle OD, McKinstry HA (1967) Temperature dependence of the elastic constants of the alkali halides. I. NaCl, KCl, and KBr. *J Appl Phys* 38:437–446
- Spetzler HA, Yoneda A (1993) Performance of the complete travel-time equation of state at simultaneous high pressure and temperature. *Pure Appl Geophys* 141:379–392
- Spetzler H, Sammis CG, O'Connell RJ (1972) Equation of state of NaCl: ultrasonic measurements to 8 kbar and 800°C and static lattice theory. *J Phys Chem Solids* 33:1727–1750
- Spinolo G, Massarotti V, Campari G (1979) A polythermal attachment for X-ray powder diffractometers. *J Phys E* 12:1059–1062
- Stacey FD, Isaak DG (2003) Anharmonicity in mineral physics: a physical interpretation. *J Geophys Res* 108:2440. doi:10.1029/2002JB002316
- Taravillo M, Baonza VG, Rubio JEF, Núñez J, Cáceres M (2002) The temperature dependence of the equation of state at high pressures revisited: a universal model for solid. *J Phys Chem Solids* 63:1705–1715
- Vinet P, Ferrante J, Rose JH, Smith JR (1987) Compressibility of solids. *J Geophys Res* 92:9319–9325
- White GK (1965) The thermal expansion of alkali halides at low temperatures. *Proc R Soc London Ser A* 286:204–217
- Yamamoto S, Ohno I, Anderson OL (1987) High temperature elasticity of sodium chloride. *J Phys Chem Solids* 48:143–151
- Yates B, Panter CH (1962) Thermal expansion of alkali halides at low temperatures. *Proc Phys Soc London* 80:373–382
- Yoneda A, Osako M, Ito E (2009) Heat capacity measurement under high pressure: a finite element method assessment. *Phys Earth Planet Int* 174:309–314